

Fiber diameter mapping of a white matter phantom using d-PFG filtered MRI

M. E. Komlosh¹, E. Ozarlan¹, M. J. Lizak², F. Horkay¹, and P. J. Basser¹
¹NICHD, NIH, Bethesda, MD, United States, ²NINDS, NIH, Bethesda, MD, United States

Introduction: Multiple scattering MR techniques, such as the double pulsed gradient spin echo (d-PFG), are powerful tools to measure cell and fiber diameters¹. Recently, measurements of cell and fiber diameters of radish, spinal cord and corticospinal tract as well as a pack of beads were reported using multiple scattering MRI sequences²⁻⁴. However, what was lacking in these and previous studies was a well characterized MR phantom with which to validate these measurements and a modeling framework that relates the MR sequence parameters and material microstructure to the MR signal attenuation profile. In this study we measured the pore diameter of a glass capillary array (GCA) phantom using d-PFG filtered MRI⁵ sequence and analyzed the result using a model that accounts for partial volume effects and incorporates the actual d-PFG sequence parameters.

Materials and Methods: The phantom consists of two water-filled GCA wafers (Photonis); nominal pore diameter=10 μ m; thickness=500 μ m. d-PFG-filtered MRIs were performed by applying the two wave vectors sequentially (with no mixing period). The angle between them, ϕ , was varied between 0° and 360°. A 7T vertical-bore Bruker DRX system was used with PFG parameters: $\delta=3.15$ ms, $\Delta=50$ ms, and G between 0 and 295mT·m⁻¹ and imaging parameters: TR/TE = 7000/12ms, FOV=20mm and slice thickness = 1mm. The separation between the d-PFG and imaging blocks (ST) were 1.3ms and 20.8ms, respectively. The technique introduced in ref. 6 was used to estimate the pore diameter by calculating the MR signal attenuation due to restricted diffusion within packed cylinders comprising the GCA. This method involves a necessary extension of the multiple correlation function (MCF) framework⁷. The simulations account for a free water compartment^{8,9}, diffusion and imaging gradients. A pixel-by-pixel analysis was applied to create a pore diameter map. Light microscopy was used as the “gold standard” to measure the GCA’s pore diameter.

Results and Discussion: Figure 1a presents a d-PFG filtered MRI image of a GCA using $G=295$ mT·m⁻¹. Fig. 1b shows the experimental and simulated data for all values of G and ϕ . Table 1 lists the estimated pore diameters. Simulations fit the data very well and the MRI pore diameter estimates are within 3% of optical measurements. Optical microscopy measurements of a similar GCA yielded a pore diameter=9.3 μ m. Note that the effect of the imaging gradients on the data depends on the separation time between the two blocks. Figure 1c shows the inner diameter distribution map of the GCA phantom, scaled such that 8.5 μ m is black and 10 μ m is white. The uniform intensities throughout the image indicate a tight pore diameter distribution across the phantom.

Conclusions: d-PFG filtered MRI is a powerful tool for pore diameter measurements and mapping applications. We have successfully demonstrated and validated this MR technique on a highly ordered pack of glass microcapillaries using light microscopy. The pore diameter estimation method accounts for the salient independent experimental parameters. We obtained the first quantitative compartment size map of a controlled specimen using d-PFG filtered MRI. The inner diameter image suggests the potential for this new contrast mechanism as a sensitive means to probe local material microstructure.

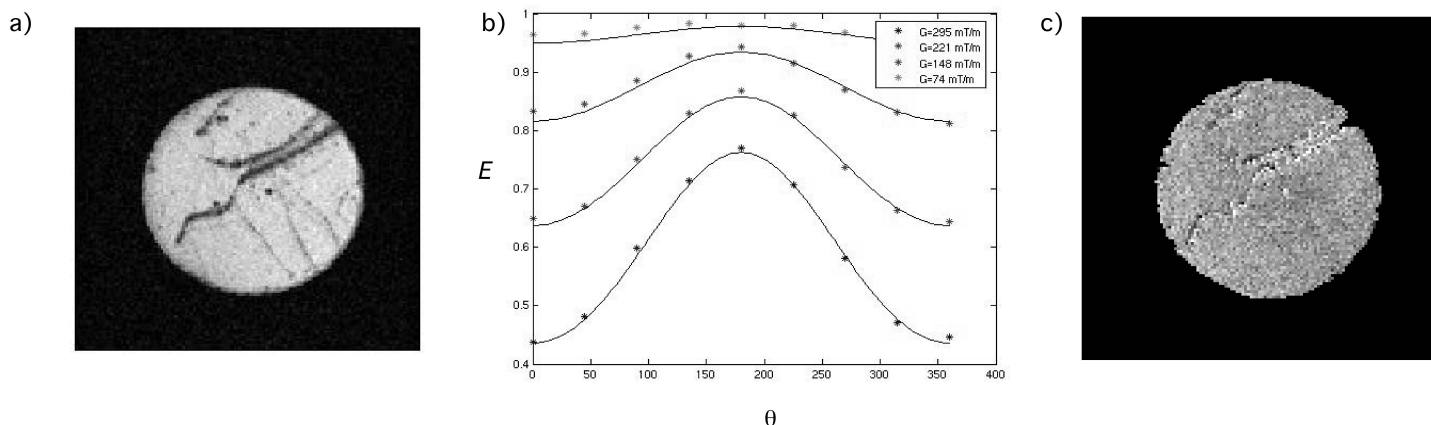


Figure 1: a) d-PFG filtered MRI image of a GCA using $G=295$ mT·m⁻¹. b) experimental and simulated data for all values of G and ϕ . c) d-PFG filtered MRI inner diameter distribution map. ST= 1.3ms

Table 1:

G (mT/m)	d_1 (μ m)	d_{1g} (μ m)	d_2 (μ m)	d_{2g} (μ m)
74	9.2 ± 0.8	9.0 ± 0.7	9 ± 1	9 ± 1
149	9.6 ± 0.2	9.4 ± 0.2	9.4 ± 0.2	9.4 ± 0.2
221	9.39 ± 0.09	9.30 ± 0.09	9.26 ± 0.07	9.26 ± 0.07
295	9.41 ± 0.07	9.35 ± 0.07	9.42 ± 0.05	9.42 ± 0.05

d_1 and d_2 – pore diameter estimation for ST=1.3 and 20.8ms imaging gradient neglected

d_{1g} and d_{2g} – same as above with imaging gradients taken into consideration.

1. Y. Cheng et al. *J Am Chem Soc*, **121**, 7935 (1999). 2. M. A. Koch, et al. *Magn Reson Med*, **60**, 90 (2008). 3. Webber, et al *Magn Reson Med* **61**, 1001(2009) 4. M. A. Koch, et al. *Proceeding ISMRM* **16**, 764, (2008) 5. Komlosh et al., *Magn Reson Med*, **59**, 803, (2008). 6. Ozarlan et al., *J Chem Phys*, **130**, 104702, (2009) 7. Grebenkov, *Rev Mod Phys*, **79**, 1077, (2007). 8. Ozarlan et al., *J Chem Phys*, **128**, 154511, (2008). 9. Shemesh et al. *J Magn Reson* **200**, **214**, (2009).